UNITED NATIONS UNIVERSITY
GEOTHERMAL TRAINING PROGRAMME
Orkustofnun, Grensasvegur 9,
IS-108 Reykjavik, Iceland

Reports 2011
Number 19

WELL TEST INTERPRETATION AND PRODUCTION PREDICTION FOR WELL SD-01 IN THE SKARDDALUR LOW-TEMPERATURE FIELD, SIGLUFJÖRDUR, N-ICELAND

Liu Junrong
China University of Petroleum
No. 66 Changjiang West Road
Huangdao District, Qingdao City
Shandong Province, 266555
CHINA
junrliu@upc.edu.cn

ABSTRACT

Recently a tunnel was constructed between Siglufjördur and Ólafsfjördur in central N-Iceland, which passes through the groundwater system in the mountains above the Skútudalur low-temperature geothermal field. Afterwards, the water level in Skútudalur reservoir started to drop. In order to ensure the geothermal water supply for the coming years, a new well named SD-01 was drilled in the Skarddalur field, which is located to the west of the Skútudalur field. After drilling, two step-rate tests and one long term production test were conducted in SD-01 to observe its pressure response to production. The data were analysed by using WellTester, Lumpfit and the multiple rate test method. The permeability thickness of the Skarddalur geothermal system is estimated to be around 10 Dm, the skin factor of the well between –1.2 and –1.5, the productivity index around 5-6 (L/s)/bar and the reservoir thickness in the range of 200-240 m. The permeability thickness results from the three methods are quite similar. Based on the present long term production and build-up data, a three-tank open model was developed and the reservoir seems to be a combination of an inner confined system and an unconfined recharge system. Using LUMPFIT, the water level was also predicted for the coming 10 years for different production rates.

1. INTRODUCTION

Siglufjördur is among the northernmost towns in Iceland, located at the foot of towering mountains on the shore of a small fjord with the same name. It has about 1600 residents at present. Fishing, marine product processing and related services are the main industries in the town. Siglufjördur has rich low-temperature geothermal resources and has been heated by a geothermal district heating system since 1978.

The Skútudalur area is the main low-temperature geothermal field in Siglufjördur, located on the east side of the Siglufjördur fjord, serving the town of Siglufjördur on the west side of the fjord. The geothermal water temperature of this system is about 70°C and the average production rate is around

20 L/s. This is not a highly productive system, but it does reach equilibrium during constant production (Axelsson et al., 2010).

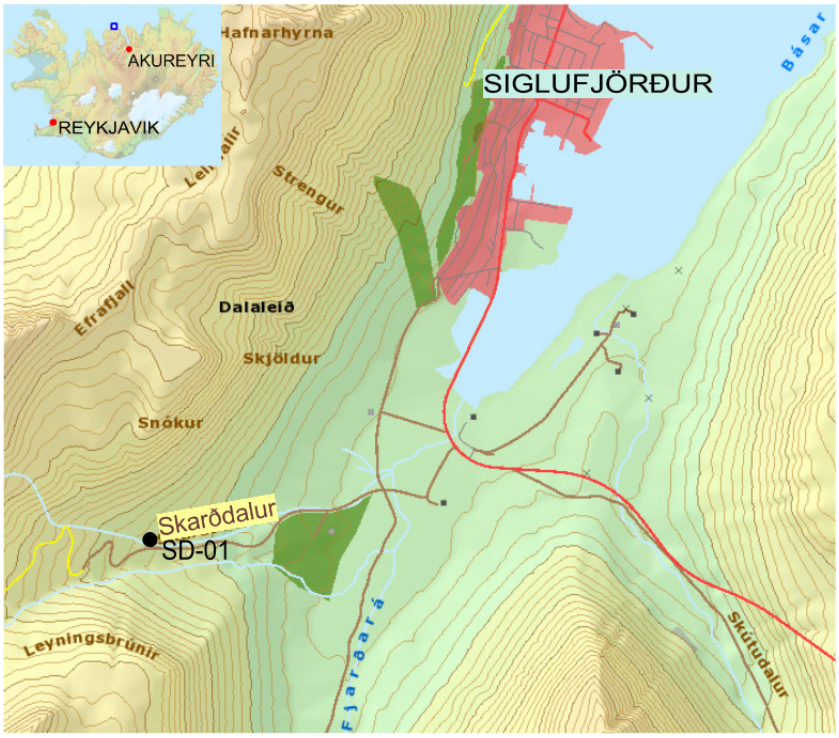

FIGURE 1: Location of Skarddalur in Siglufjördur, N-Iceland (Landmaelingar Íslands, 2011)

In order to improve transportation in this area, a 3.9 km long tunnel connecting Siglufjördur with Ólafsfjördur, a town which lies southeast of Siglufjördur, was under construction from September 2006 to March 2008 (Axelsson and Ólafsson, 2010). The tunnel passes through the groundwater system in the mountains above Skútudalur, which supposedly supports the pressure for the Skútudalur geothermal system. After this, the water level in the Skútudalur reservoir started to drop (Axelsson et al., 2010).

Given this state of the water level in the Skútudalur geothermal system and in order to ensure plenty of hot water supply for coming decades, a new production well named SD-01 was drilled at Skarddalur in September, 2010. Skarddalur is located to the west of Skútudalur, in a valley to the southwest, cutting the mountainous area between Snókur in the north and Leyningsbrúnir in the south (Figure 1). Before drilling SD-01, 12 exploration wells had been drilled in Skarddalur, the deepest one being 360 m deep (Figure 2). The last temperature gradient well, SF-16, suggested the existence of a 70°C reservoir system under Skarddalur, recorded in the well below around 300 m depth. Based on the temperature data from these 12 gradient wells, the well site for SD-01 was selected by ÍSOR (Iceland GeoSurvey) and the well was drilled by Jardboranir hf (Iceland Drilling Company Ltd.) in September 2010. The well is owned and operated by RARIK, Iceland State Electricity.

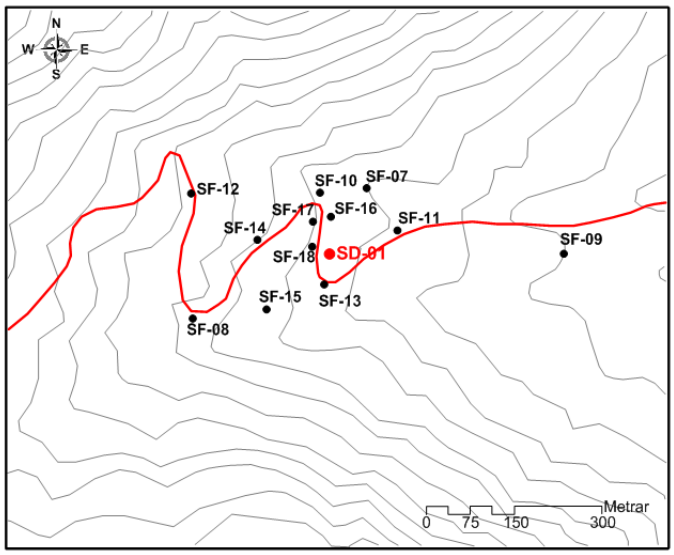

FIGURE 2: SF-temperature gradient wells and the production well SD-01 in the Skarddalur field (Kristinsson and Egilsson, 2010)

The well was completed at 702 m depth. It was cased down to 286 m with a 10¾" steel casing and drilled with an 8½" drill bit down to the bottom. Temperature logging after the drilling showed that there are several feed zones in the well with the two main ones at 302 and 480 m depth, as may be seen in Figure 3. The figure shows inter-zonal flow of 73°C water from 480 m to the feed point at 300 m. Down-hole video recordings from the well also showed that there are some smaller feed-

zones under the first main one at 302 m, such as at around 387, 444, 478/480, 483 and 510 m depth. It indicates that the well follows a fracture from around 444 down to 520 m and water from the fracture enters the well in different sections. It seems that these feed-zones belong to the same geothermal system. The geological layers are very similar to each other and mainly consist of tholeiitic lava layers intersected by some red inter-beds. The main alteration minerals are quartz and calcite (Jóhannesson, et al., 2010; Kristinsson and Egilsson, 2010).

After the drilling, a draw down step-test was performed with the drilling string blowing out air at different depths, thereby helping the water to flow. It was estimated that 30 L/s could be pumped from the well at a temperature of 72-73°C (Kristinsson and Egilsson, 2010). A long term production test was conducted from 16 May to 25 July, 2011, and then the well was shut-in for recovery, lasting up to 25 August, 2011. During the production period, the second step-test was conducted on 31 May, 2011.

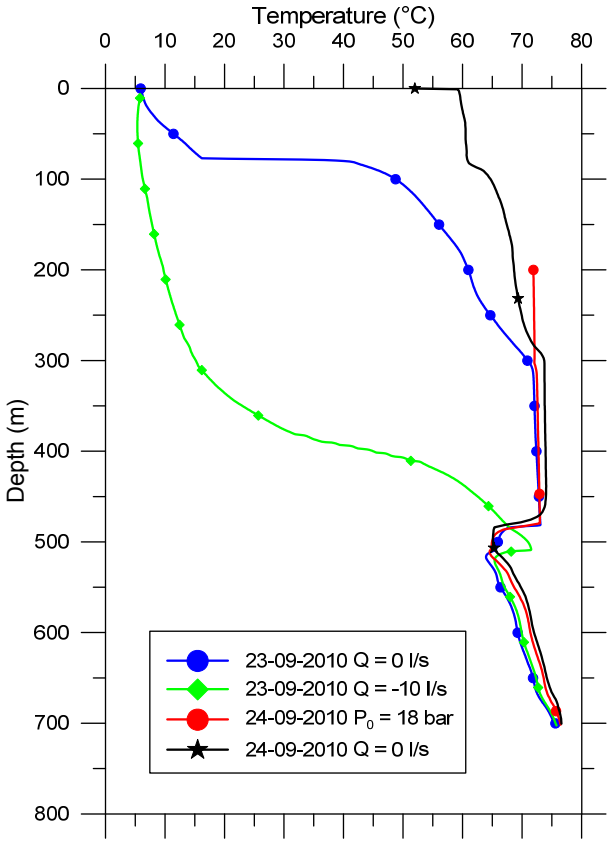

FIGURE 3: Temperature profiles in well SD-01

In order to understand the reservoir potential and plan its sustainable development, the well test data from the first and second production step-tests, as well as the production history and recovery period, were studied based on well test theory, and with lumped parameter modelling. The results are described in the following parts. The theoretical background is first described to provide deeper knowledge of the subject. Afterwards the data processing, modelling and results are discussed, including 10 year prediction scenarios. Finally, the conclusions are presented.

2. THEORETICAL BACKGROUND

2.1 Well testing

Well testing is a very important way to understand the properties of a hydrological reservoir and the conditions in the wellbore in question. In most well test cases, the pressure response of a given reservoir, due to production or injection in a well, is monitored at the same well or at adjacent observation wells. Through the well testing, the conditions of a well, its flow capacity and reservoir properties can be evaluated with the most appropriate model. Among the important parameters of well test interpretation are permeability-thickness and formation storage coefficient of the reservoir.

Well test analysis is, in fact, synonymous with a pressure transient analysis. Pressure transients are caused by changes in production or injection of fluids; hence, the flow rate is treated as a transient input and the pressure as a transient output (Horne, 1995). Usually, the traditional well test interpretation method does not consider the effects of temperature change during the test. On the other hand, the temperature often changes in reality due to variations in the injection or flow rate, so the density of the water changes and, therefore, affects the pressure. Under these conditions, a combination of the pressure response and the temperature change may give a more reasonable result.

2.1.1 Pressure diffusion equation

The basic equation of well testing theory is the pressure diffusion equation. The most commonly used solution of the pressure diffusion equation is the Theis solution or the line source solution. Three governing laws are needed in deriving the pressure diffusion equation (Jónsson, 2011):

- *Conservation of mass inside a given control volume:*

$$Mass\ flow\ in - Mass\ flow\ out\ = (\rho Q)_{r+dr} - (\rho Q)_r$$
$$= Rate\ of\ change\ of\ mass\ within\ the\ control\ volume$$
$$\left(\rho Q + \frac{\partial(\rho Q)}{\partial r}dr\right) - \rho Q = 2\pi r dr \frac{\partial(\varphi\rho h)}{\partial t}$$
$$\frac{\partial(\rho Q)}{\partial r} = 2\pi r \frac{\partial(\varphi\rho h)}{\partial t} \tag{1}$$

- *Conservation of momentum, expressed by Darcy's law for radial flow towards the well:*

$$Q\ =\ 2\pi r h \frac{k}{\mu}\frac{\partial P}{\partial r} \tag{2}$$

where Q = Volumetric flow rate [m^3/s];
h = Reservoir thickness [m];
k = Formation permeability [m^2];
P = Reservoir pressure [Pa];
r = Radial distance [m] ; and
μ = Dynamic viscosity of fluid [Pa·s].

- *Fluid compressibility:*

$$c_f\ =\ \frac{1}{\rho}\left(\frac{\partial\rho}{\partial P}\right)_T \tag{3}$$

where c_f = Compressibility of fluid [Pa^{-1}];
ρ = Density of fluid [kg/m^3]; and
T = Temperature [°C].

Additionally, some simplifying assumptions are needed:

- Isothermal flow;
- Homogeneous and isotropic reservoir;
- Production well completely penetrating the reservoir thickness;
- Reservoir completely saturated with single-phase fluid.

Based on these equations and assumptions, the pressure diffusion equation can be expressed as:

$$\frac{1}{r}\frac{\partial}{\partial r}\left(\frac{r\partial P(r,t)}{\partial r}\right)\ =\ \frac{\mu c_t}{k}\left(\frac{\partial P(r,t)}{\partial t}\right) = \frac{S}{T}\frac{\partial P(r,t)}{\partial t} \tag{4}$$

where c_t = Total compressibility of rock and water, $\phi c_f + (1-\phi)c_r$, [Pa^{-1}];
c_f = Compressibility of fluid, [Pa^{-1}];
c_r = Compressibility of rock, [Pa^{-1}];
ϕ = Porosity, [-];
S = Storativity, $c_t h$, [$m^3/(Pa\cdot m^2)$] ;
T = Transmissivity, kh/μ, [$m^3/(Pa\cdot s)$];

h = Effective reservoir thickness, [m];
k = Permeability of the rock, [m^2];
μ = Dynamic viscosity of the fluid, [Pa·s];
$P(r,t)$ = Reservoir pressure at a distance *r* and time *t* [Pa]; and
t = Time [s].

2.1.2 Theis solution

The radial pressure diffusion equation is a partial differential equation. To solve this equation, initial and boundary conditions are required. For an infinite acting reservoir, the initial and boundary conditions are (Jónsson, 2011):

a) *Initial conditions*

$$P(r,t) = P_i \; for \; t = 0 \; and \; for \; all \; r > 0 \tag{5}$$

where P_i = initial reservoir pressure [Pa].

b) *Boundary conditions*

$$P(r,t) \rightarrow P_i \; for \; r \rightarrow \infty \; and \; for \; all \; t > 0 \tag{6}$$

$$2\pi rh\frac{k}{\mu}\frac{\partial P}{\partial r} \rightarrow Q \; for \; r \rightarrow 0 \; and \; for \; all \; t > 0 \tag{7}$$

The solution to the radial diffusion equation with these boundary and initial conditions is given by:

$$P(r,t) = P_i - \frac{Q\mu}{4\pi kh}W\left(\frac{\mu c_t r^2}{4kt}\right) = P_i - \frac{Q}{4\pi T}W\left(\frac{Sr^2}{4Tt}\right) \tag{8}$$

where $W(x)$ is the well function or the exponent integral function defined as:

$$W(x) = -E_i(-x) = \int_x^{\varphi}\left(\frac{e^{-u}}{u}\right)du$$

For small values of x, i.e. $x < 0.01$, $W(x) \approx -ln(x) - \gamma \approx -ln(x) - 0.5772$, where γ is the Euler constant. Therefore, if:

$$t > 25\frac{\mu c_t r^2}{k} = 25\frac{Sr^2}{T}$$

The Theis solution can be expressed as:

$$P(r,t) = P_i + \frac{2.303\,Q}{4\pi T}\left[log\left(\frac{Sr^2}{4Tt}\right) + \frac{\gamma}{2.303}\right] \tag{9}$$

Equation 9 is the most used equation in well test analysis and describes pressure at a distance r at time t when producing at constant rate Q in a radial flow of a single-phase fluid in a homogeneous reservoir model.

2.1.3 Semi-logarithmic well test analysis

By monitoring pressure changes with time, it may be possible to fit the observed pressure history to the theoretical results and identify two important parameter groups, the permeability-thickness (kh) and the storativity ($c_t h$). By rearranging Equation 9, the solution can be written as

$$\Delta P = P_i - P(r,t) = \frac{2.303\,Q}{4\pi T} log\left(\frac{2.246\,T}{Sr^2}\right) + \frac{2.303\,Q}{4\pi T} log(t) \quad (10)$$

The above equation is in the form of $\Delta P = \alpha + mlog(t)$. Plotting ΔP vs. $log(t)$ gives a semi-log straight line response for the infinite acting radial flow period of a well, and this is referred to as a semi-log analysis. The line is characterized by slope m and an intercept α, where

$$\Delta P = P_i - P(r,t),\ \alpha = \frac{2.303\,Q}{4\pi T} log\left(\frac{2.246\,T}{Sr^2}\right),\ m = \frac{2.303\,Q}{4\pi T}$$

By determining m, the formation transmissivity can be estimated by

$$T = \frac{kh}{\mu} = \frac{2.303\,Q}{4\pi m} \quad (11)$$

If the temperature is known, then the dynamic viscosity μ can be found from steam tables, thus the permeability-thickness (kh) can be calculated as follows:

$$kh = \frac{2.303\,Q\mu}{4\pi m} \quad (12)$$

And the storativity can be obtained as

$$S = c_t h = 2.246\left(\frac{kh}{\mu}\right)\left(\frac{t}{r^2}\right) 10^{-\frac{\Delta P}{m}} = 2.246\,T\left(\frac{t}{r^2}\right) 10^{-\frac{\Delta P}{m}} \quad (13)$$

The semi-log analysis is based on the location and interpretation of the semi-log straight line response that represents the infinite acting radial flow behaviour of the well. However, as the wellbore has a finite volume, it becomes necessary to determine the duration of the wellbore storage effect and the time at which the semi-log straight line begins (Horne, 1995).

Pressure propagation does not take place uniformly throughout the reservoir because it is affected by local heterogeneities. Usually, due to the inappropriate pressure control during drilling or completion, some external fluids (such as mud, cement) invaded the original formation around the well and formed a zone with lower permeability. Some methods (such as acidizing, hydraulic fracturing) are often used to stimulate the reservoir so that a permeability improved zone can be formed during production. Such zones are called skin zones. It causes an additional pressure drop ΔP_s near the wellbore in addition to the normal reservoir pressure change due to production (Horne, 2010).

$$\Delta P_s = \frac{Q\mu}{2\pi kh} \times s \quad (14)$$

where s = Skin factor [-].

A negative skin factor indicates that the near well permeability is improved while a positive skin factor indicates that the near well surroundings are damaged. The skin due to a damaged zone of radius r_s and reduced permeability k_s can be calculated from:

$$s = \left(\frac{k}{k_s} - 1\right) ln\frac{r_s}{r_w} \quad (15)$$

where k = permeability of undamaged zone [m^2];
k_s = permeability of damaged zone [m^2];
r_s = radius of damaged zone [m]; and
r_w = radius of wellbore [m].

Since the skin has a similar effect as changing the effective radius of the well, the effective well radius is r_{weff} given by:

$$r_{weff} = r_w e^{-s} \tag{16}$$

In a well with skin, the total pressure changes at the well are given by:

$$\Delta P = P_i - P(r_w, t) \approx \frac{2.303\,Q}{4\pi T}\left[log(t) + log\left(\frac{T}{S r_w^2}\right) + 0.3514 + 0.8686\,s\right] \tag{17}$$

The skin effect does not change the evaluation of permeability-thickness in a semi-log analysis, but it does influence the evaluation of storativity as shown in the following equation:

$$Se^{-2s} = c_t h e^{-2s} = 2.246\,T\left(\frac{t}{r^2}\right)10^{-\frac{\Delta P}{m}} \tag{18}$$

2.1.4 Derivative plot

A derivative plot is a useful diagnostic tool for examining the effects of wellbore storage, recharge and barrier boundaries, leakage, a delayed gravity response and fracture flow. The derivative plot provides a simultaneous presentation of $log(\Delta P)\ vs.\ log(\Delta t)$ and $log(tdP/dt)\ vs.\ log(\Delta t)$ and provides many separate characteristics in one plot that would otherwise require different plots. Selecting an appropriate calculation method of derivative is very important when performing a derivative analysis. A straightforward numerical differentiation using adjacent points will produce a very noisy derivative (Horne, 1995).

$$t\left(\frac{\partial P}{\partial t}\right) = t_i\left[\frac{(t_i - t_{i-1})\Delta P_{i+1}}{(t_{i+1} - t_i)(t_{i+1} - t_{i-1})} + \frac{(t_{i+1} + t_{i-1} - 2\,t_i)\Delta P_i}{(t_{i+1} - t_i)(t_i - t_{i-1})} - \frac{(t_{i+1} - t_i)\Delta P_{i-1}}{(t_i - t_{i-1})(t_{i+1} - t_{i-1})}\right] \tag{19}$$

where t is the time, P is the pressure, and index $(i-1)$ and $(i+1)$ refer to the two adjacent points to i.

If the data are distributed in a geometric progression, then the numerical differentiation with the logarithm of time can be used to remove noise from the calculations (Horne, 1995).

$$t\left(\frac{\partial P}{\partial t}\right) = \left[\frac{ln(t_i/t_{i-1})\Delta P_{i+1}}{ln(t_{i+1}/t_i)ln(t_{i+1}/t_{i-1})} + \frac{ln(t_{i+1} \times t_{i-1}/{t_i}^2)\Delta P_i}{ln(t_{i+1}/t_i)ln(t_i/t_{i-1})} - \frac{ln(t_{i+1}/t_i)\Delta P_{i-1}}{ln(t_i/t_{i-1})ln(t_{i+1}/t_{i-1})}\right] \tag{20}$$

If this method still leads to a noisy derivative, the best method to reduce the noise is to use data points that are separated by at least 0.2 of a log cycle. Hence:

$$t\left(\frac{\partial P}{\partial t}\right) = \left[\frac{ln(t_i/t_{i-k})\Delta P_{i+j}}{ln(t_{i+j}/t_i)ln(t_{i+j}/t_{i-k})} + \frac{ln(t_{i+j} \times t_{i-k}/{t_i}^2)\Delta P_i}{ln(t_{i+j}/t_i)ln(t_i/t_{i-k})} - \frac{ln(t_{i+j}/t_i)\Delta P_{i-k}}{ln(t_i/t_{i-k})ln(t_{i+j}/t_{i-k})}\right] \tag{21}$$

where $ln(t_{i+j}) - ln(t_i) \geq 0.2$; and

$ln(t_i) - ln(t_{i-k}) \geq 0.2$

The value of 0.2 (known as the differentiation interval) could be replaced by smaller or larger values (usually between 0.1 and 0.5), with consequent differences in the smoothing of the noise.

2.1.5 Multiple - rate test analysis

For a drawdown test, most analysis methods require a constant flow rate; however, it is often impractical or impossible to maintain a constant rate long enough to complete a drawdown test. In such cases, multiple (variable) rate testing and analysis techniques may be used. A multiple-rate test may range from one with an uncontrolled, variable rate, to one with a series of constant rates (Bourdet, 2002). The introduction of more than one rate in a well-test sequence causes additional pressure transients to be introduced into the reservoir. The second flow rate superimposes a second pressure transient on the first and both continue to move outward in the reservoir as production continues. Such processes continue till the pressure response corresponding to the final rate stabilizes.

Unlike pressure build-up tests, multiple-rate testing provides test data while production continues and tends to minimize changes in the wellbore storage coefficient. Accurate flow rate and pressure measurements are essential for the successful analysis of any pressure transient well test. Rate measurements are much more critical in multiple-rate testing than in conventional, constant-rate well tests.

In this method, the variable rates are divided into several steps, i.e. each pumping period is divided into several time intervals. The changes of the flow rate in each interval are assumed to be very small and the flow rate can be treated as a constant. As shown in Figure 4, the pumping process is divided into n time intervals, with the flow rate of the i^{th} time interval being q_i. For a confined aquifer which was pumped at variable discharge rates, the expression for the drawdown in the aquifer at time t during the n^{th}pumping period can then be obtained by applying the superposition principle. It should be mentioned that the method of lumped parameter modelling (Section 2.2) applied in this work also assumes a variable flow-rate and is based on the superposition principle.

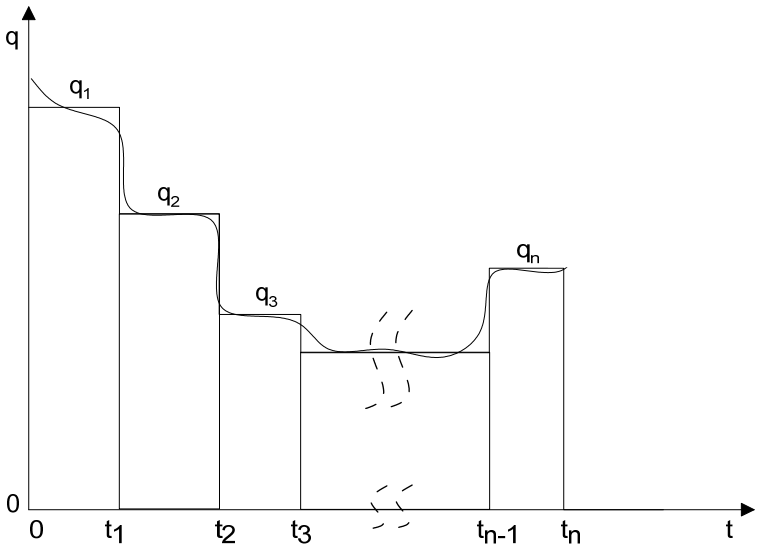

FIGURE 4: Schematic figure of multiple rate production

For the first time interval:

$$p(t) = p_i - \frac{2.303\,q_1}{4\pi T}\left[log\left(\frac{2.246T}{Sr^2}\right) + log(t)\right] \quad (0 < t \leq t_1) \tag{22}$$

For the second time interval:

$$p(t) = p_i - \frac{2.303\,q_2}{4\pi T}\left[log\left(\frac{2.246T}{Sr^2}\right) + \frac{q_1}{q_2}log(t) + \frac{(q_2 - q_1)}{q_2}log(t - t_1)\right] \; ; \; (t_1 < t \leq t_2) \tag{23}$$

With the same method, at the n^{th} time interval:

$$p(t) = p_i - \frac{2.303\,q_n}{4\pi T}\left[log\left(\frac{2.246\,T}{Sr^2}\right) + \sum_{j=1}^{n}\frac{(q_j - q_{j-1})}{q_n} log(t - t_{j-1})\right] \; ; \; (t_{n-1} < t \leq t_n) \quad (24)$$

where $t_0 = 0;\ q_0 = 0$.

This equation is a linear equation with the form $y = A - mx$, where:

$$y = p(t) \text{ and } x = \sum_{j=1}^{n}\frac{(q_j - q_{j-1})}{q_n} log(t - t_{j-1}) \quad (25)$$

The slope is:

$$m = \frac{2.303\,q_n}{4\pi T} = \frac{2.303\,\mu q_n}{4\pi kh} \quad (26)$$

Then the transmissivity T and permeability thickness kh can be estimated when the reservoir temperature and pressure are known.

The pressure axis intercept is given by:

$$A = p_i - \frac{2.303\,q_n}{4\pi T}\left[log\left(\frac{2.246\,T}{Sr^2}\right)\right] \quad (27)$$

Assuming that the initial pressure p_i is known, the storativity S can be found as

$$S = \frac{2.246\,T}{r^2} \times 10^{-\frac{p_i - A}{m}} \quad (28)$$

2.2 Lumped parameter modelling

Reservoir modelling plays a very important role in the sustainable development and management of geothermal resources. Through reservoir modelling, we can obtain information on the physical conditions, the nature and properties of the reservoir, predict the reservoir response to future production, as well as estimate the production potential and the outcome of different development plans. Various modelling methods are used in the geothermal industry, such as simple analytical modelling, lumped parameter modelling and detail numerical modelling.

In a simple model, the real structure and spatially varying properties of a geothermal system are greatly simplified, properties are assumed constant. Such models can only simulate one parameter, such as pressure, temperature or chemistry, not two or more simultaneously. The detailed numerical model can accurately simulate complex geometry and structure, also variable properties. Such models can simulate pressure, temperature (enthalpy) and chemistry simultaneously.

Lumped parameter models ignore geometry and integrate all the properties into lumped values. The method applied here treats the simulations as an inverse problem and automatically fits the response functions of the lumped models to the observed data. It may be used to simulate water level/pressure change data and can simulate long and detailed data very accurately. Compared to detailed numerical models, lumped parameter modelling is not very time consuming and does not require many field data (Axelsson et al., 2005). The model assumes isothermal flow behaviour and does not account for the changes in temperature with time. In reality, the temperature variations can be substantial when there are injection operations in a field, or when natural recharge is at a significantly different temperature from the present local reservoir temperature.

2.2.1 Lumped parameter models

A general lumped parameter model is shown in Figure 5. It consists of a few tanks (capacitors) that are connected by flow resistors (conductors). The tanks simulate the storage capacity of different parts of the reservoir and the resistors or conductors simulate the permeability. A tank in a lumped model has a storage coefficient (capacitance) κ when it responds to a load of liquid mass m with a pressure increase $\mathrm{P} = \mathrm{m}/\kappa$. The resistors (conductors) simulate the flow resistance in the reservoir, controlled by the permeability of the rocks. The mass conductance (inverse of resistance) of a resistor is σ when it transfers $\mathrm{Q} = \sigma\Delta\mathrm{P}$ units of liquid mass per unit time at the pressure difference ΔP. The pressures in the tanks simulate the pressures in different parts of the reservoir, whereas production from the reservoir is simulated by withdrawal of water from only one of the tanks (Axelsson, 1989).

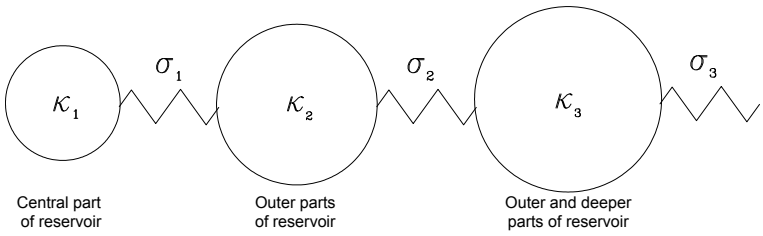

FIGURE 5: A general lumped parameter model used to simulate water level or pressure changes in a geothermal system (Axelsson et al., 2005)

Lumped models can be either open or closed. Open models are connected by a resistor to an infinitely large imaginary reservoir which maintains a constant pressure, and it can be considered optimistic since equilibrium between production and recharge is eventually reached and the water level will stabilize during long term production. On the other hand, closed lumped models are isolated from any external reservoir and can be considered pessimistic since no recharge is allowed for such models and the water level declines steadily with time during long term production. Actual reservoirs can most generally be represented and simulated by two- or three-tank closed or open lumped parameter models (Axelsson, 1989). The pressure response, P, of a single-tank open model for production Q, assuming a step response since time $t = 0$, is given by the following equation (Axelsson and Arason, 1992):

$$P(t) = -\left(\frac{Q}{\sigma_1}\right)\left(1 - e^{\frac{\sigma_1 t_i}{\kappa_1}}\right) \tag{29}$$

The pressure response of a more general open model with N tanks, to Q assuming a step response, from time $t = 0$, is given by

$$P(t) = -\sum_{j=1}^{N} Q\left(\frac{B_j}{L_j}\right)\left(1 - e^{-L_j \times t_i}\right) \tag{30}$$

The pressure response of a general closed model with N tanks is given by

$$P(t) = -\sum_{j=1}^{N} Q\left(\frac{B_j}{L_j}\right)\left(1 - e^{-L_j \times t_i}\right) + Q \times C \times t_i \tag{31}$$

The coefficients B_j, L_j and C are functions of the storage coefficients of the tanks (κ_j) and the conductance coefficients of resistors (σ_j) of the model, and can be estimated by the LUMPFIT program, which uses an iterative non-linear inversion technique to fit a corresponding solution to observed pressure or water level (Axelsson, 1989).

2.2.2 Estimation of reservoir properties based on model results

After developing a model which matches the observed data very well with LUMPFIT, the size and properties of the different parts of the reservoir can be estimated by the conductance and capacitance coefficients obtained from the model (Vitai, 2010).

The surface area of the different parts of the system A_j can be calculated by the following equation

$$A_j = \frac{\kappa_j}{S \cdot h} \tag{32}$$

where κ_j = Storage coefficient or capacitance [kg/Pa] or [m·s^2];
S = Storativity of the reservoir [kg/(Pa·m^3)] or [s^2/m^2] ;
h = Reservoir thickness [m]; and
j = 1, 2, 3, referring to the innermost, the deeper or outer and the recharge part of the reservoir, respectively, (this is valid only for a 3-tank model; for a 1-tank model $j = 1$, and for a 2-tank model $j = 1{,}2$).

The storativity depends on the storage mechanism and therefore differs for confined and unconfined reservoirs. For a confined liquid-dominated reservoir, it can be expressed as:

$$S = \rho_w[\phi c_w + (1-\phi)c_r] \tag{33}$$

For an unconfined reservoir, in the case where the capacitance is controlled by the mobility of a free surface, the storativity is:

$$S = \phi/(g \cdot h) \tag{34}$$

Conductance σ_j can be used to estimate the permeability k_j (or permeability thickness $k_j h_j$) of the different parts of the reservoir. For a 1-dimensional flow, it can be calculated as:

$$k_j = (\sigma_j L_j \upsilon)/A_{\perp j} \tag{35}$$

where k_j = Permeability of the reservoir [m^2];
υ = Kinematic viscosity of the geothermal fluid [m^2/s];
σ_j = Conductance coefficients of resistor [m·s] or [kg/(Pa·s)];
$A_{\perp j}$ = Area of the reservoir perpendicular to the flow path [m^2]; and
L_j = Length of the flow path between adjacent reservoir parts, of the outermost part of the system and the surroundings [m].

For 2- dimensional flow, the permeability can be expressed as:

$$k_j = \left(\sigma_j \upsilon ln\frac{r_{j+1}}{r_j}\right)/2\pi h_j \tag{36}$$

where r_j = defined in Table 1; and
h_j = thickness of the reservoir [m].

For 3- dimensional flow, the permeability can be calculated by:

$$k_j = \left[\sigma_j \upsilon \left(\frac{1}{r_j} - \frac{1}{r_{j+1}}\right)\right]/4\pi \tag{37}$$

The radius of each tank and the equations to calculate distances from the centre to the relevant edge are listed in Table 1. The tanks in LUMPFIT may be thought of as concentric where R_1 is the radius of the innermost one, R_2 of the second one and R_3 of the outermost one. In the formulas in Table 1, r_1, r_2, r_3 and r_4 are the distances from the centre to the relevant edge.

TABLE 1: The radius of each tank and equations to calculate distances from the centre to the relevant edge for different models, for 2-dimensional flow

Model type	Equations
1-tank open model	$r_1 = R_1/2; r_2 = 3\,R_1/2$
2-tank closed model	$r_1 = R_1/2; r_2 = R_1 + (R_2 - R_1)/2$
2-tank open model	$r_1 = R_1/2; r_2 = R_1 + (R_2 - R_1)/2; r_{2+1} = R_2 + (R_2 - R_1)/2$
3-tank closed model	$r_1 = R_1/2; r_2 = R_1 + (R_2 - R_1)/2; r_3 = R_2 + (R_3 - R_2)/2$
3-tank open model	$r_1 = R_1/2; r_2 = R_1 + (R_2 - R_1)/2; r_3 = R_2 + (R_3 - R_2)/2; r_4 = R_3 + (R_3 - R_2)/2$
	$V_1 = \kappa_1/S; V_2 = \kappa_2/S; V_3 = \kappa_3/S;$ $R_1 = (V_1/\pi h)^{0.5};$ $R_2 = [(V_1 + V_2)/\pi h]^{0.5}; R_3 = [(V_1 + V_2 + V_3)/\pi h]^{0.5}$ where V_j is the volume of the jth tank [m^3] and R_j is the radius of the first j tanks combined [m].

3. WELL TEST PROCESS FOR WELL SD-01

3.1 Test process

After drilling, the first production step-test (drawdown test) was performed on 24 September, 2010 and lasted 8 hours. The drilling string was lowered first to 120 m, then to 150 m and finally to 190 m and air compressors were used to pump the well by air-lift. The flow of hot water was measured in a V-notch weir box and the pressure was recorded in the well at 300 m depth. The corresponding flow rates from the well were approximately 12, 17 and 26 L/s; near-equilibrium in the pressure response was achieved except for the recovery stage where the flow rate was 0 L/s. The temperature logged at 300 m reached 72.2 °C and was increasing slightly during the flow test. The initial static water level in the reservoir was measured at 84 m depth (Kristinsson and Egilsson, 2010).

A long term production test and a recovery period were conducted in well SD-01 and the water levels were monitored in the SF-exploration wells that are in the vicinity of the well SD-01 (Figure 2). The water levels in the SF-exploration wells did not change much (Table 2). It seems that the production from well SD-01 has no effects on the observation wells around it and the well seems to be located in an isolated aquifer system, but this needs to be further confirmed. Because all of the SF-observation wells are shallow wells, they may only connect to the shallower groundwater system but not the deeper geothermal system.

TABLE 2: Water level depth (in m) monitored in several SF-observation wells

Date / Well	16 May	17 May	18 May	19 May	20 May
SF-7	6.5	6.5	6.5	6.44	6.4
SF-8	8.57	8.57	8.6	8.53	8.47
SF-9	4.94	4.95	5.01	4.6	4.47
SF-12	18.23	18.24	18.34	18.3	18.28
SF-14	42.4	42.39	42.36	42.34	42.34
SF-17	6.79	6.79	6.84	6.72	6.62

During the long term production test, a second production step-test (drawdown test) was performed on 31 May 2011, lasting about 14 hours. A total of fourteen steps were observed. The temperature and pressure were measured at 180 m depth during the test.

3.2 Initial test results

3.2.1 First production step-test

Figure 6 shows the measured flow rate, pressure and temperature during the first production test with three drawdown steps when drilling strings blew out air at 120, 150 and 190 m depth in the well during the steps, respectively, and the last step, a recovery step, after the air blowing had been stopped. The flow rate had some variations during each step and each step only lasted a very short time. During drilling, the water table in the borehole was generally at around 78–80 m depth. The data from the pressure gauge show that the water table was at 84 m depth when the test began. During the step test, the well produced around 12 L/s when blowing the air from the drilling string at 120 m depth, 17 L/s with the drilling string at 150 m and 26 L/s with the drilling string at 190 m. The data from the pressure sensor at 300 m depth indicated that the water level reached a good equilibrium during the first three steps but not in the fourth step, the recovery step; it needed more time. The performance profile of the well and the fitting results are shown in Figure 7. From the curve fitting, it seems that there is some turbulence effect in the well, even though that is hard to determine accurately.

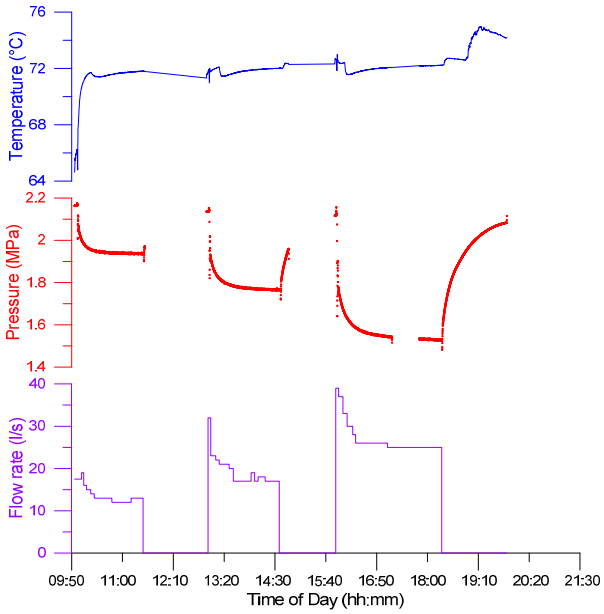

FIGURE 6: Measured flow rate, pressure and temperature during the first production step-test of well SD-01

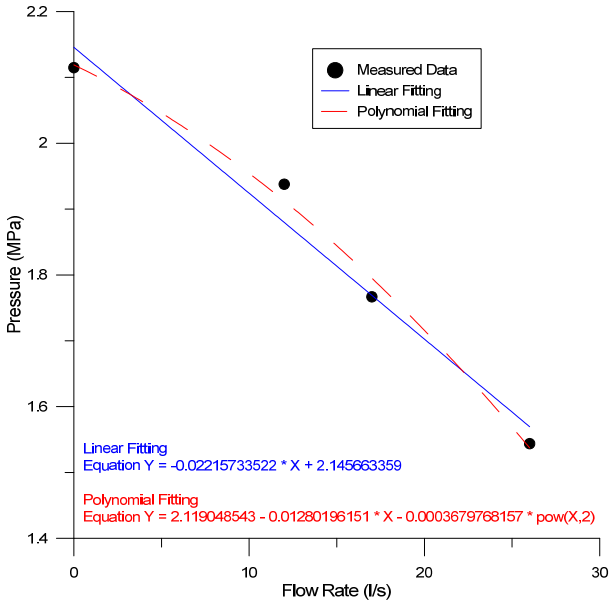

FIGURE 7: Stabilized pressure against flow rate and fitting curves for the first production step-test

3.2.2 Second production step-test

Figure 8 shows the measured flow rate, pressure and temperature during the second production step test. During the test, the temperature increased when the flow rate decreased. The performance profile of the well and the fitting results are shown in Figure 9. The fitting results show that there is a small difference between the linear and polynomial fittings. It seems, therefore, that there is very little turbulence effect in the well.

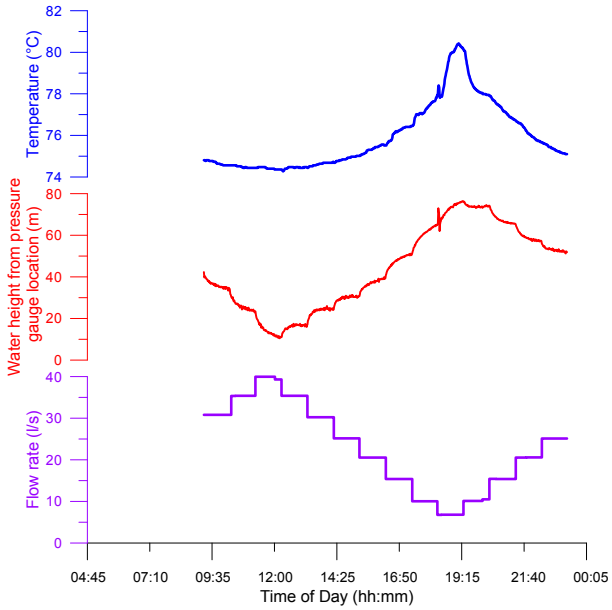

FIGURE 8: Measured flow rate, water height above the pressure gauge and temperature during the second production step-test

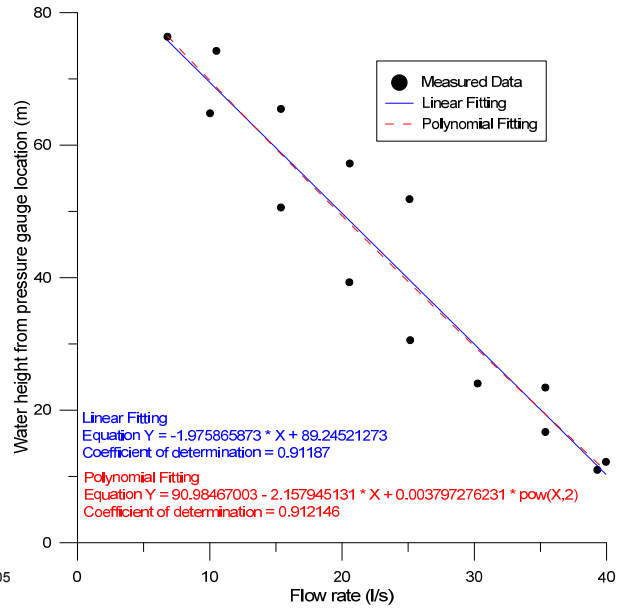

FIGURE 9: The water height above the pressure gauge against flow rate and fitting curves for the second production step-test

3.2.3 Long term production test

The long term production test lasted from 16 May to 25 July, 2011, i.e. 71 days, at about 25 L/s, except for the second step-test. The well was closed on 26 July for recovery which lasted for 31days. During this period, a variable rate test (referred to as the second production step-test in this paper) was performed with fourteen steps on 31 May 2011. The production rate was measured at the surface and the pressure was recorded with a down-hole pressure gauge located at 180 m depth. The pressure was converted to water level and the production history is shown in Figure 10.

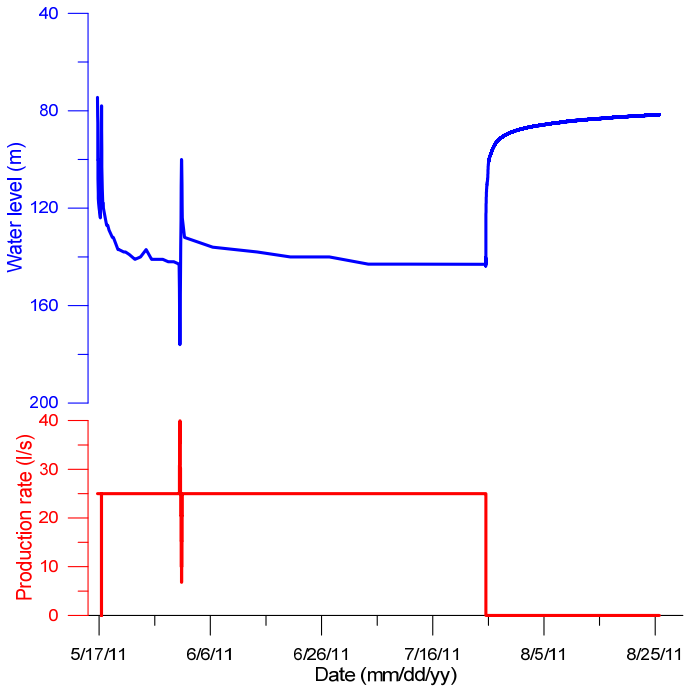

FIGURE 10: Long term production test data for well SD-01

4. STEP TEST INTERPRETATION

4.1 Interpretation of the first production step-test

4.1.1 WellTester interpretation

To model the test data (pressure against time) during the first production step-test, software called WellTester was used, developed by ÍSOR – Iceland GeoSurvey (Júlíusson et al., 2007). The initial input parameters used in WellTester are shown in Table 3.

TABLE 3: Initial parameters used in the WellTester analysis

Parameter name	Parameter value
Estimated reservoir temperature [°C]	72.2
Estimated reservoir pressure [bar]	21.6
Wellbore radius [m]	0.108
Porosity [%]	10
Dynamic viscosity of reservoir fluid [Pa·s]	0.000393
Total compressibility [1/Pa]	2.19×10^{-10}

To get better fitting with WellTester, the data was separated into four parts (steps). One of the reasons is that the data for each step are measured at different air blowout depths and the recovery data between each step is missing. The average flow rates (12, 17, 26 and 0 L/s for each step), which were taken from the measurements, were used to fit the model. Each step was modelled separately and the reservoir parameters were calculated. By trying different flow models to fit each of the steps with WellTester, the best flow model is the homogeneous reservoir, constant pressure boundary model, with constant skin and wellbore storage. The output parameters are listed in Table 4 and the output plots of each step with sampled data and model results are shown in Figures 11-14.

TABLE 4: Summary of the results from WellTester for the first production step-test of well SD-01

Parameter name	Step 1	Step 2	Step 3	Step 4
Transmissivity [m^3/(Pa·s)]	3.3×10^{-8}	3.6×10^{-8}	3.7×10^{-8}	2.2×10^{-8}
Storativity [m^3/(Pa·m^2)]	4.4×10^{-8}	4.8×10^{-8}	5.1×10^{-8}	6.0×10^{-8}
Skin factor [-]	–1.4	–1.5	–1.2	–3.6
Wellbore storage [m^3/Pa]	7.9×10^{-6}	6.4×10^{-6}	8.2×10^{-6}	5.0×10^{-5}
Productivity index [(L/s)/bar]	5.9	5.1	4.5	5.4
Effective permeability [mD] *	63	64	64	33
Reservoir thickness [m]	205	220	235	275
Permeability thickness [Dm]*	13	14	15	9

* 1 D ≈ 1×10^{-12} m^2, D = Darcy

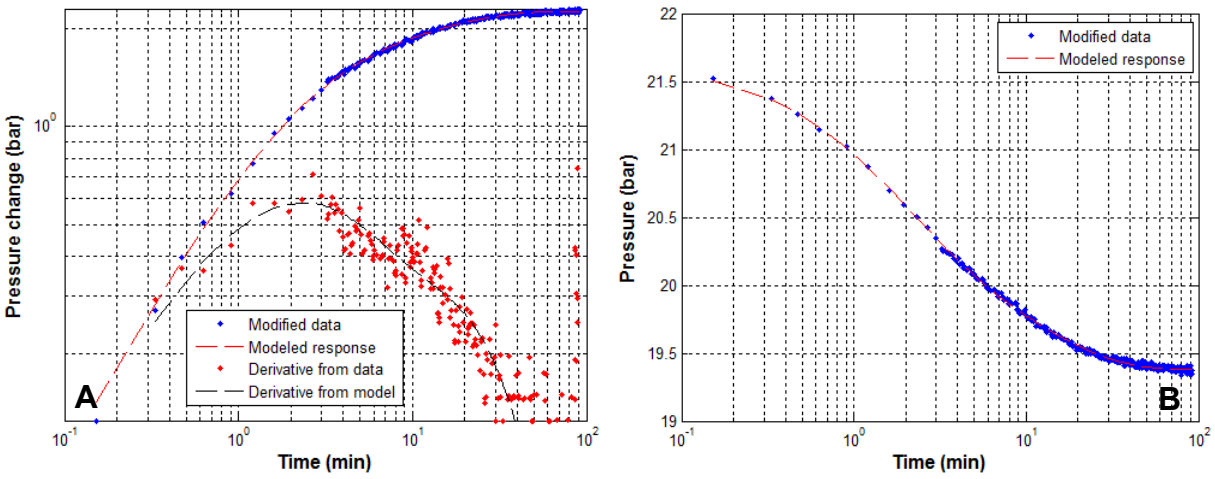

FIGURE 11: Step 1 – a) Pressure change (above) and derivative of pressure (below) against time on a log-log scale for sampled and modelled data during the first production step-test; b) Pressure change against time on a log-linear scale for sampled and modelled data during the first production step-test

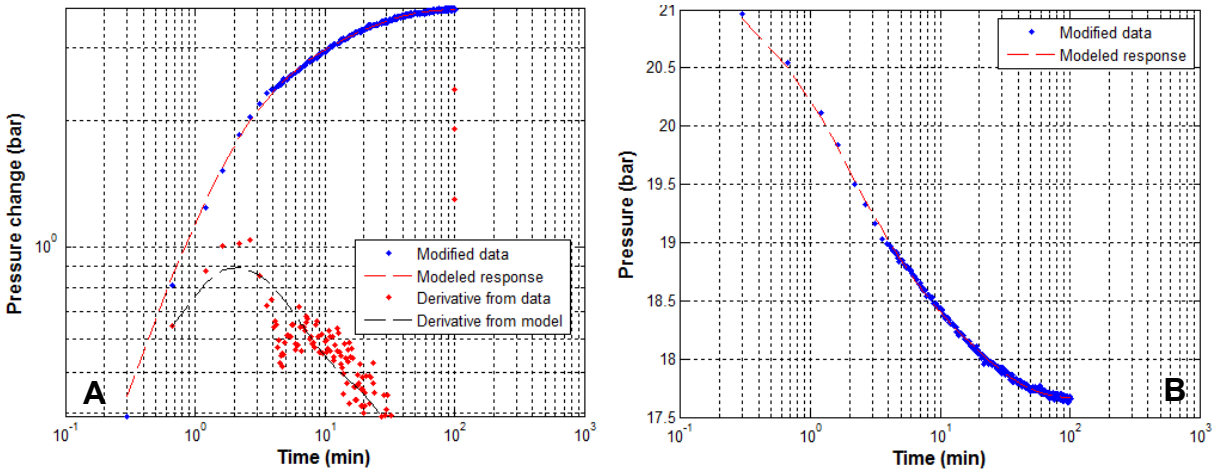

FIGURE 12: Step 2 – a) Pressure change (above) and derivative of pressure (below) against time on a log-log scale for sampled and modelled data during the first production step-test; b) Pressure change against time on a log-linear scale for sampled and modelled data during the first production step-test

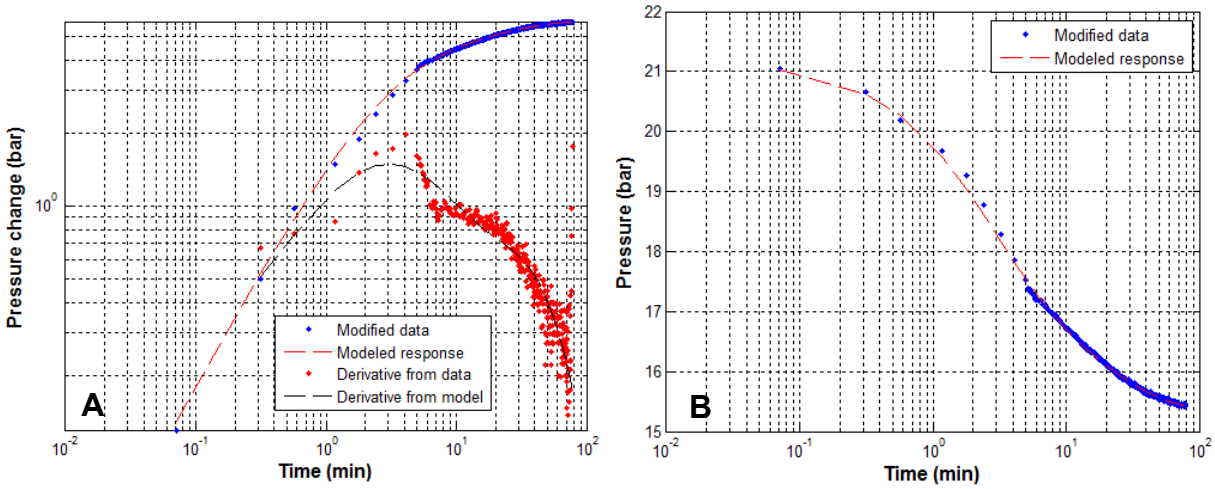

FIGURE 13: Step 3 – a) Pressure change (above) and derivative of pressure (below) against time on a log-log scale for sampled and modelled data during the first production step-test; b) Pressure change against time on a log-linear scale for sampled and modelled data during the first production step-test

From Figures 11-14, it can be seen that the selected flow model fits well for each step. The parameters in Table 4 show that the values found for the different steps were typical for the values found in Iceland. Because the data is missing between the steps, all the steps were not modelled together. Also it needs to be noted that the parameters of the first three steps are quite close to each other. Based on these three steps, the skin factor can be assumed to be between -1.2 and -1.5, the reservoir thickness is around 200-240 m, the productivity index around 5-6 (L/s)/bar, the permeability about 64 mD and the permeability thickness around 13-15 Dm. The estimated reservoir thickness is also very close to the results of temperature logging.

4.1.2 LUMPFIT interpretation

The LUMPFIT software was developed by Axelsson and Arason (1992) at Orkustofnun – National Energy Authority, the research department which became ÍSOR 8 years ago. LUMPFIT was used to match the production test data and to estimate the reservoir properties in this work. The idea behind

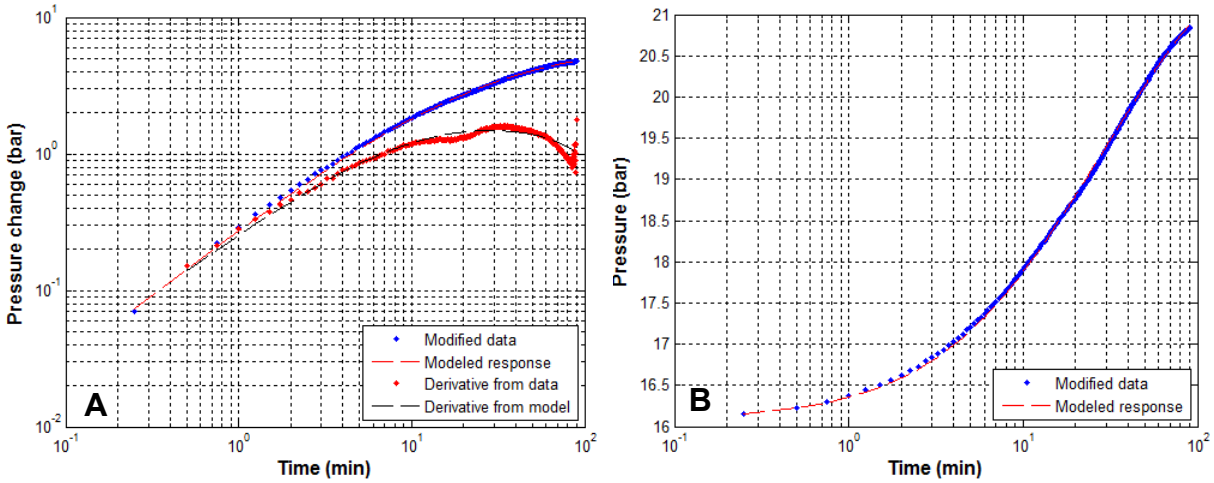

FIGURE 14: Step 4 – a) Pressure change (above) and derivative of pressure (below) against time on a log-log scale for sampled and modelled data during the first production step-test; b) Pressure change against time on a log-linear scale for sampled and modelled data during the first production step-test

this is that LUMPFIT can obtain reservoir parameters through history matching from the observed data as well as calculate future reservoir pressure predictions.

During the history matching, different turbulence coefficients were used to compare with the fitting results (Figure 7) and to determine the turbulence effect in the well. Additionally, the effect of variations in the flow rate within a step was analysed since it had been difficult to keep the flow rate constant during each step. Therefore, variable rate matching and constant rate matching for each step were also conducted to evaluate the effects of the flow rate on the processing method.

Using LUMPFIT with the step-test, a two-tank open model was successfully developed as a best fit to the observed data. For the variable rate case, the observed and simulated data using a two-tank open model with different turbulence coefficients are shown in Figures 15-18.

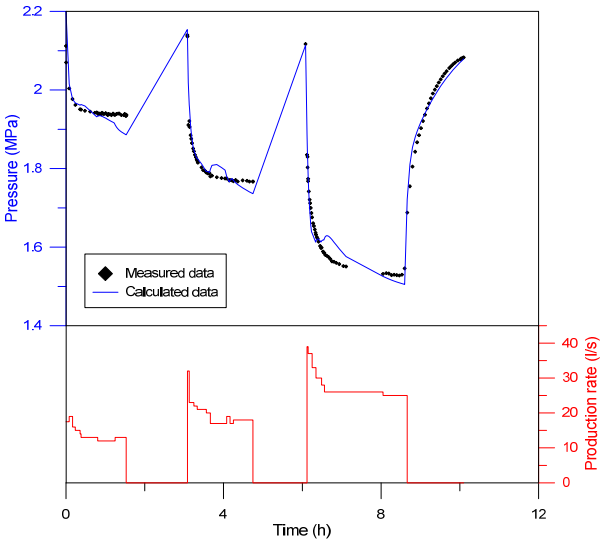

FIGURE 15: Observed pressure and production rate and simulated results with turbulence coefficient = 0 MPa/(L/s)^2, against time for the first production step-test

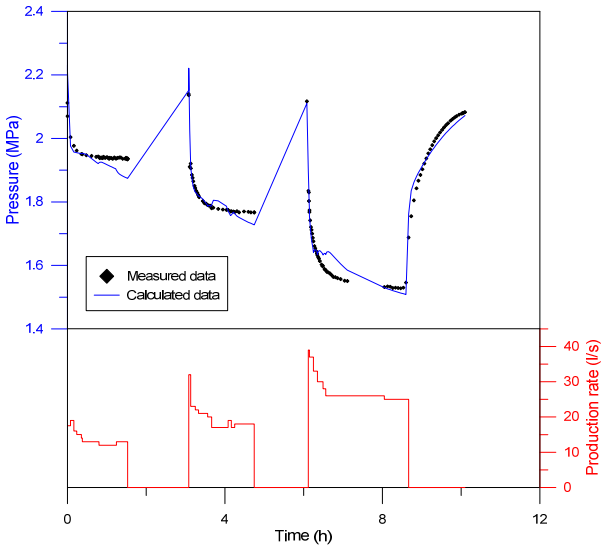

FIGURE 16: Observed pressure and production rate and simulated results with turbulence coefficient = 0.001 MPa/(L/s)^2, against time for the first production step-test

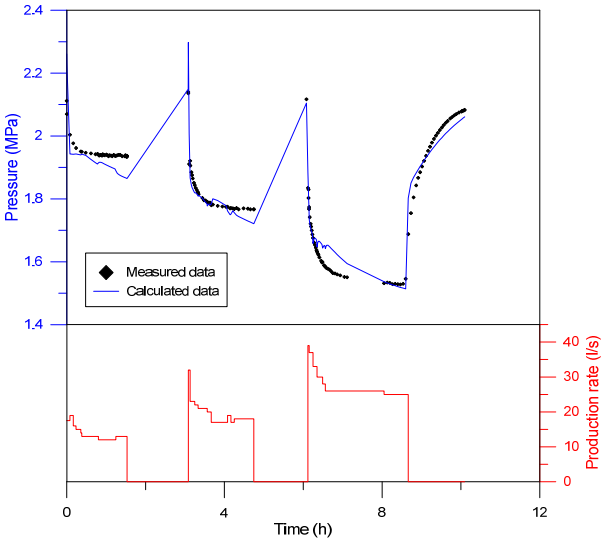

FIGURE 17: Observed pressure and production rate and simulated results with turbulence coefficient = 0.002 MPa/(L/s)^2, against time for the first production step-test

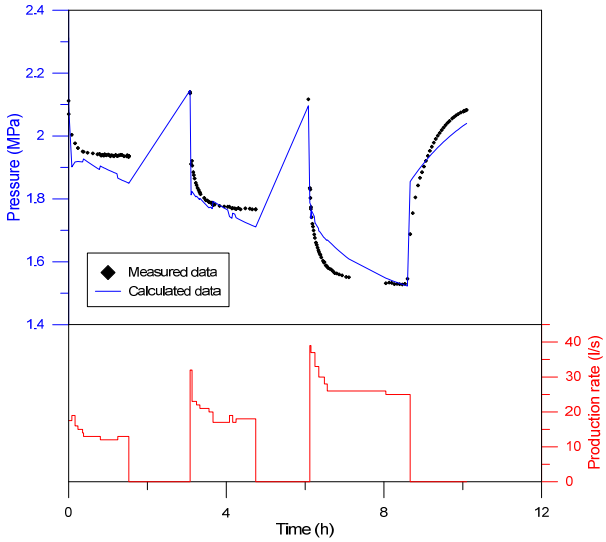

FIGURE 18: Observed pressure and production rate and simulated results with turbulence coefficient = 0.00368 MPa/(L/s)^2, against time for the first production step-test

The matching results for the constant rate in each step are shown in Figures 19-22. The output parameters by LUMPFIT and calculated permeability thickness with Equation 36 are listed in Tables 5 and 6, respectively. The kinematic viscosity of the water was taken as 3.9×10^{-7} m^2/s.

Comparing Figures 15-18 and Figures 19-22, it can be seen that the variable rate case matches better than the constant rate case with the same turbulence coefficient. So it is more reasonable to use the actual flow rate rather than the average flow rate for each step when using LUMPFIT. From the diagrams, it can be seen that the best matching is the one with no turbulence in the well. The results seem to contradict the fitting results (Figure 7), but when considering the diagrams and parameters in Tables 5 and 6, we have reason to believe that there is no (or very small) turbulence effect in the well. The permeability thickness of the first tank is estimated at about 7 Dm. The results are of the same order of magnitude as the WellTester results.

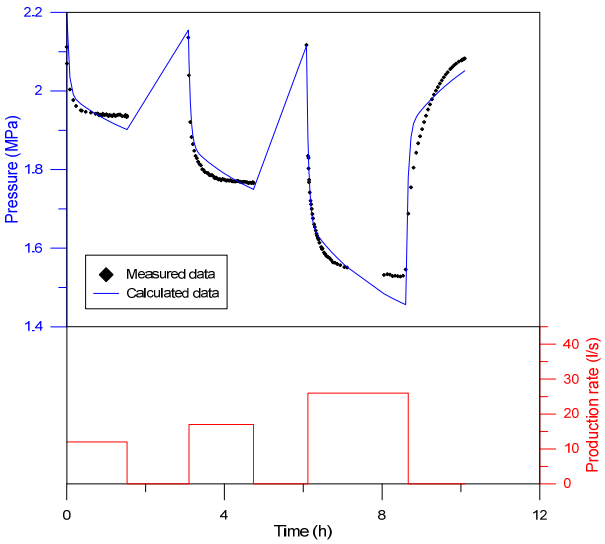

FIGURE 19: Observed pressure and production rate and simulated results with turbulence coefficient = 0 MPa/(L/s)^2, against time for the first production step-test

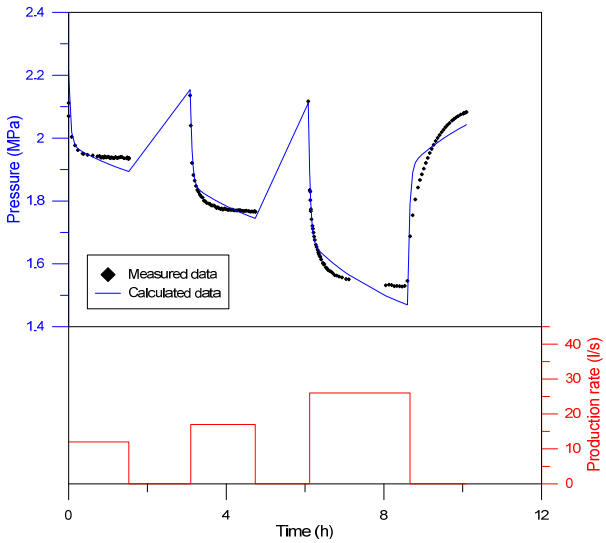

FIGURE 20: Observed pressure and production rate and simulated results with turbulence coefficient = 0.001 MPa/(L/s)^2, against time for the first production step-test

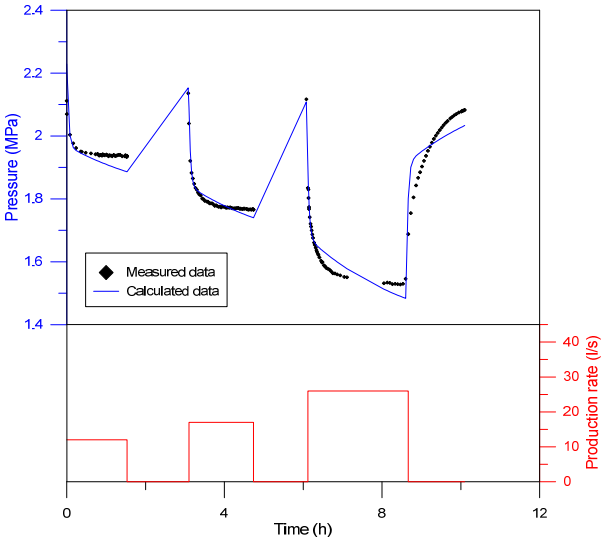

FIGURE 21: Observed pressure and production rate and simulated results with turbulence coefficient = 0.002 MPa/(L/s)^2, against time for the first production step-test

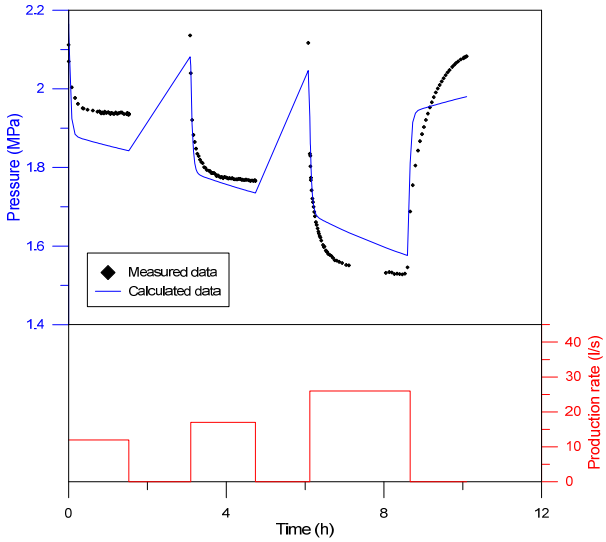

FIGURE 22: Observed pressure and production rate and simulated results with turbulence coefficient = 0.00368 MPa/(L/s)^2, against time for the first production step-test

TABLE 5: Lumped parameter model results for variable flow rate in the first production step-test

Parameter name	**Turbulence coefficient (MPa/(L/s)^2)**			
	0	**0.001**	**0.002**	**0.00368**
Capacitance κ_1 [kg/Pa]	1.7×10^{-2}	9.2×10^{-3}	5.3×10^{-3}	5.4×10^{-4}
Capacitance κ_2 [kg/Pa]	0.3	0.3	0.3	0.4
Conductance σ_1 [m·s]	7.0×10^{-5}	6.3×10^{-5}	5.5×10^{-5}	4.4×10^{-5}
Conductance σ_2 [m·s]	6.4×10^{-5}	6.0×10^{-5}	5.9×10^{-5}	5.7×10^{-5}
Coefficient of determination R^2 [%]	96.9	96.5	96.0	96.0
Reservoir volume V_1 [m^3]	3×10^{5}	2×10^{5}	8×10^{4}	8×10^{3}
Reservoir volume V_2 [m^3]	4×10^{6}	4×10^{6}	5×10^{6}	6×10^{6}
Permeability thickness k_1h_1 [D·m]	7	7	7	9
Permeability thickness k_2h_2 [D·m]	3	3	3	4

TABLE 6: Lumped parameter model results for constant flow rate in the first production step-test

Parameter name	**Turbulence coefficient (MPa/(L/s)^2)**			
	0	**0.001**	**0.002**	**0.00368**
Capacitance κ_1 [kg/Pa]	1.1×10^{-2}	8.5×10^{-3}	6.8×10^{-3}	6.4×10^{-3}
Capacitance κ_2 [kg/Pa]	0.5	0.6	0.6	1.4
Conductance σ_1 [m·s]	5.5×10^{-5}	4.9×10^{-5}	4.4×10^{-5}	4.1×10^{-5}
Conductance σ_2 [m·s]	6.8×10^{-5}	6.5×10^{-5}	6.3×10^{-5}	7.3×10^{-5}
Coefficient of determination R^2 [%]	95.6	96.3	96.5	92.9
Reservoir volume V_1 [m^3]	2×10^{5}	1×10^{5}	1×10^{5}	1×10^{5}
Reservoir volume V_2 [m^3]	8×10^{6}	8×10^{6}	9×10^{6}	2×10^{7}
Permeability thickness k_1h_1 [D·m]	7	7	6	7
Permeability thickness k_2h_2 [D·m]	4	4	4	5

4.2 Interpretation of the second production step-test

4.2.1 LUMPFIT interpretation

For the second step-test, LUMPFIT was also used to match the raw test data. A two-tank open model was successfully developed as for the first test. Figures 23-26 show the measured data and the simulated data of a two-tank open model with different turbulence coefficients. The output parameters by LUMPFIT and the calculated permeability thickness with Equation 36 are listed in Table 7.

Comparing Figures 23-26, it can be seen that the best match is when there is no turbulence in the well. The permeability thickness of the first tank is about 6 Dm, which is very close to the result of the first production step-test (about 7 Dm) from LUMPFIT.

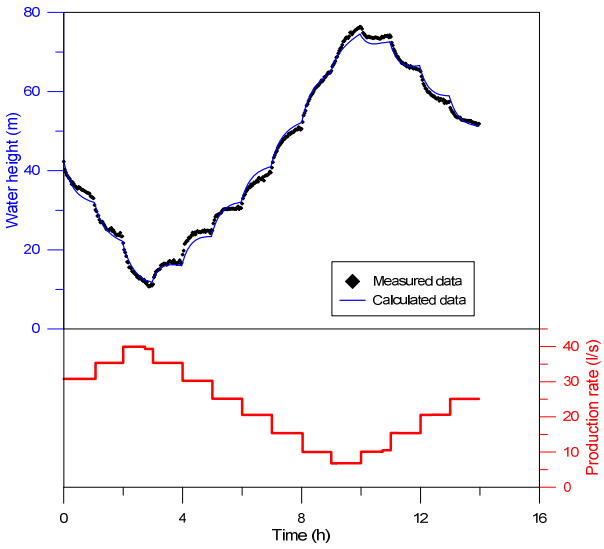

FIGURE 23: Observed water height above the pressure gauge and production rate and simulated results with turbulence coefficient = 0 m/(L/s)^2, against time for the second production step-test

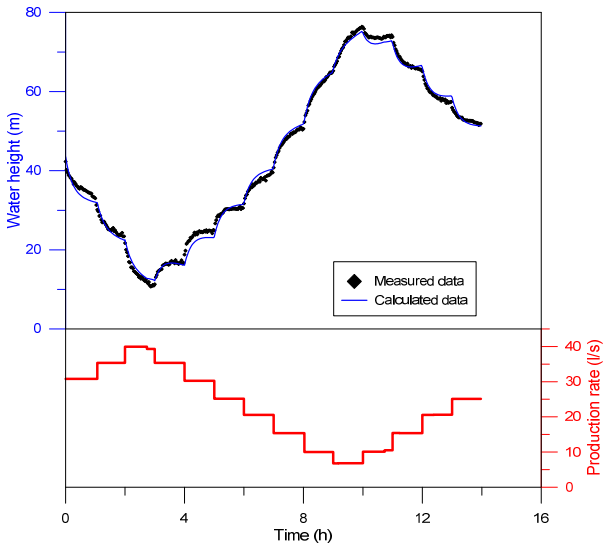

FIGURE 24: Observed water height above the pressure gauge and production rate and simulated results with turbulence coefficient = 0.00379 m/(L/s)^2, against time for the second production step-test

TABLE 7: Lumped parameter model results of the second production step-test

Parameter name	Turbulence coefficient (m/(L/s)^2)			
	0	**0.00379**	**0.01**	**0.012**
Capacitance κ_1 [kg/Pa]	6.3×10^{-2}	4.6×10^{-2}	2.9×10^{-2}	2.5×10^{-2}
Capacitance κ_2 [kg/Pa]	1.5	1.4	1.3	1.3
Conductance σ_1 [m·s]	5.7×10^{-5}	5.3×10^{-5}	4.6×10^{-5}	4.5×10^{-5}
Conductance σ_2 [m·s]	9.3×10^{-6}	6.0×10^{-6}	1.6×10^{-6}	4.2×10^{-7}
Coefficient of determination R^2 [%]	99.6	99.7	99.7	99.7
Reservoir volume V_1 [m^3]	9.4×10^{5}	6.9×10^{5}	4.3×10^{5}	3.7×10^{5}
Reservoir volume V_2 [m^3]	2.2×10^{7}	2.1×10^{7}	2.0×10^{7}	2.0×10^{7}
Permeability thickness k_1h_1 [D·m]	6	6	6	6
Permeability thickness k_2h_2 [D·m]	0.5	0.3	0.09	0.02

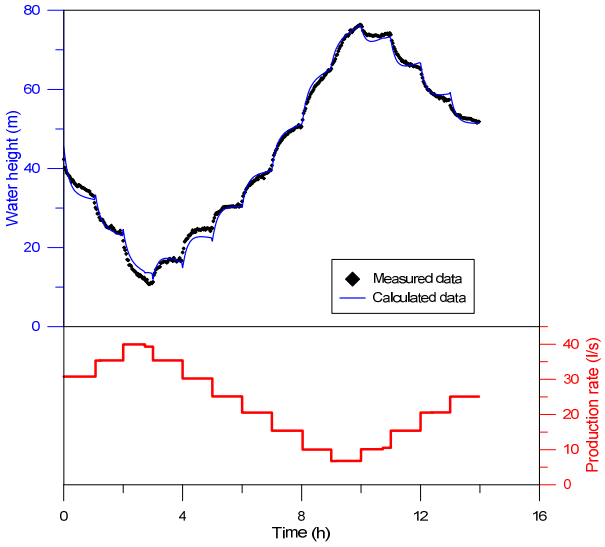

FIGURE 25: Observed water height above the pressure gauge and production rate and simulated results with turbulence coefficient = 0.01 m/(L/s)^2, against time for the second production step-test

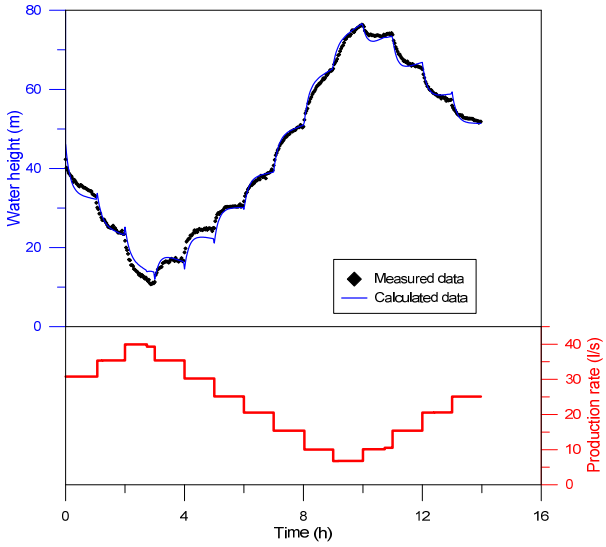

FIGURE 26: Observed water height above the pressure gauge and production rate and simulated results with turbulence coefficient = 0.012 m/(L/s)^2, against time for the second production step-test

4.2.2 Multiple - rate interpretation

The multiple rate interpretation method was also used for the second production step-test data. The diagram of $p(t)$ against $\sum_{j=1}^{n} \frac{(q_j - q_{j-1})}{q_n} log(t - t_{j-1})$ and the linear fitting results are shown in Figure 27. The linear fitting equations and the calculated permeability thicknesses are shown in Table 8. From the graphs and the calculated results, it can be seen that, except for steps 1–2 and step 14, the linear fitting curves show some similar trends, and most of the permeability thicknesses are around 6–10 D·m.

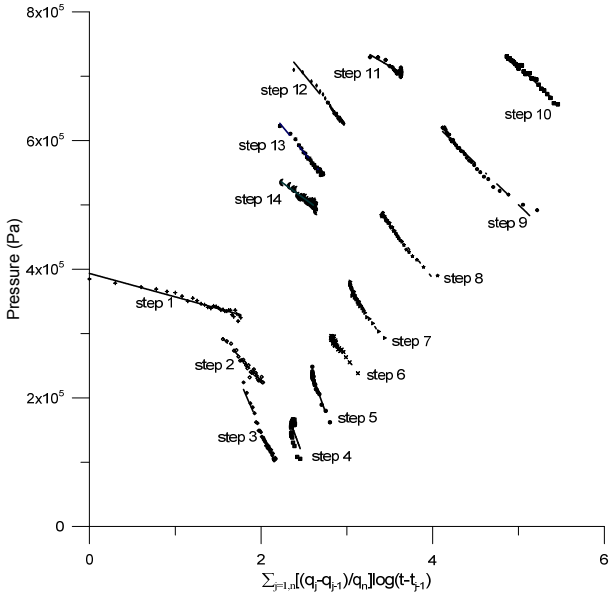

FIGURE 27: Diagram of $p(t)$ against $\sum_{j=1}^{n} \frac{(q_j - q_{j-1})}{q_n} log(t - t_{j-1})$ and linear fitting curves

4.3 Summary of the step-test results

The well test data, which were measured after drilling (first production step-test) and during a later pilot production (the second production step-test), were analysed by WellTester, LUMPFIT and using the multiple rate test analysis method. Based on the first three steps in the first production step test, the skin factor is between –1.2 and –1.5, the reservoir thickness is in the range of 200-240 m, the productivity index is about 5 (L/s)/bar and the permeability thickness is around 13-15 Dm. With LUMPFIT, the permeability thickness for the first tank is about 7 Dm. For the second production

TABLE 8: Linear fitting equations for pressure as a function of production rate and time and the calculated permeability thicknesses for the second production step test

Parameter name	Linear fitting equation	Permeability thickness [Dm]
Step 1	y = -36433.5 x + 393388.2	61
Step 2	y = -150941.9 x + 527699.1	17
Step 3	y = -308643.6 x + 767270.5	9
Step 4	y = -361310.4 x + 1008468.1	7
Step 5	y = -376931.7 x + 1214449.7	6
Step 6	y = -172942.6 x + 780373.3	11
Step 7	y = -213337.4 x + 1020335.9	7
Step 8	y = -165219.8 x + 1046856.9	7
Step 9	y = -128713.9 x + 1143743.8	6
Step 10	y = -126526.3 x + 1348234.9	4
Step 11	y = -77634.6 x + 987259.6	9
Step 12	y = -162963.5 x + 1109982.9	7
Step 13	y = -160272.8 x + 982324.9	9
Step 14	y = -96358.9 x + 751102.9	19

step-test, the permeability thickness is around 6-10 Dm by the variable rate method and about 6 Dm for the first tank from LUMPFIT; the productivity index is around 5-6 (L/s)/bar.

Based on these results, it is reasonable to conclude that the permeability thickness of the reservoir around well SD-01 is about 6-10 Dm and the productivity index around 5-6 (L/s)/bar. The LUMPFIT results for these two tests show that there is very small or no turbulence effect in the well.

5. MODELLING AND PREDICTION FOR WELL SD-01

5.1 Lumped parameter model of the field

Two lumped parameter models, a three-tank open model and a three-tank closed model, were used to simulate the observed data from the long-term production test of well SD-01, by assuming an initial water level of 74.5 m depth, average past production rate 0 L/s and a turbulence coefficient of 0. The model results are shown in Figure 28. The coefficients of determination are 95.5% for both of the

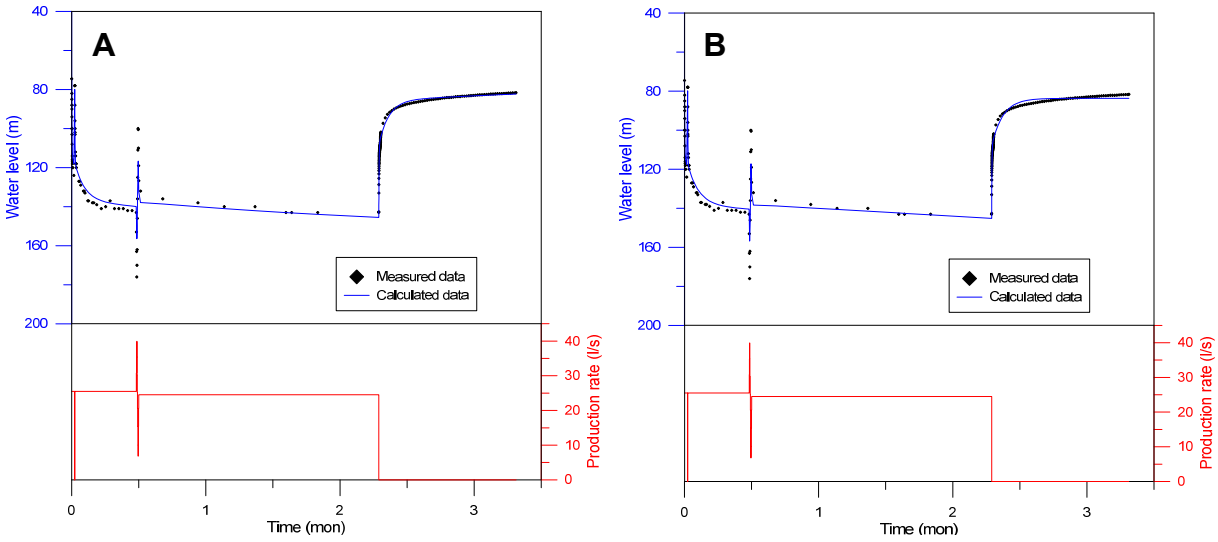

FIGURE 28: Observed and simulated water level values and production rates for well SD-01 during the long-term test, for (a) three-tank open model and (b) three-tank closed model

models. Assuming the thickness of the reservoir is about 220 m and the porosity is 10%, considering a confined and unconfined liquid-dominated system and 2-dimensional flow, the storativity, estimated surface area and permeability thickness of different parts of the reservoir have been calculated and the results are shown in Table 9.

TABLE 9: Lumped parameter model results for long term production test of well SD-01

	Three-tank open model		**Three-tank closed model**	
Capacitance κ_1 [kg/Pa]	3.3×10^{-1}		3.3×10^{-1}	
Capacitance κ_2 [kg/Pa]	21.7		22.9	
Capacitance κ_3 [kg/Pa]	951.4		1631.2	
Conductance σ_1 [m·s]	6.5×10^{-5}		6.6×10^{-5}	
Conductance σ_2 [m·s]	1.1×10^{-4}		1.0×10^{-4}	
Conductance σ_3 [m·s]	1.3×10^{-4}		-	
Coefficient of determination R^2 [%]	95.5		95.5	
	Confined	**Unconfined**	**Confined**	**Unconfined**
Storativity S [kg/(Pa·m^3)]	6.6×10^{-8}	4.8×10^{-5}	6.6×10^{-8}	4.8×10^{-5}
Reservoir volume V_1 [m^3]	5.0×10^{6}	6.9×10^{3}	5.0×10^{6}	7.0×10^{3}
Reservoir volume V_2 [m^3]	3.3×10^{8}	4.6×10^{5}	3.4×10^{8}	4.8×10^{5}
Reservoir volume V_3 [m^3]	1.4×10^{10}	2.0×10^{7}	2.5×10^{10}	3.4×10^{7}
Surface area A_1 [m^2]	2.3×10^{4}	3.1×10^{1}	2.3×10^{4}	3.2×10^{1}
Surface area A_2 [m^2]	1.5×10^{6}	2.1×10^{3}	1.5×10^{6}	2.2×10^{3}
Surface area A_3 [m^2]	6.4×10^{7}	9.1×10^{4}	1.1×10^{8}	1.5×10^{5}
Permeability thickness k_1h_1 [D·m]	9	9	9	9
Permeability thickness k_2h_2 [D·m]	13	13	14	14
Permeability thickness k_3h_3 [D·m]	7	7	-	-

5.2 Interpretation and predictions

The results from the three-tank open model and the three-tank closed model, for simulating the measured pressure and flow rate, are very similar. Because the new well SD-01 produced for about two and a half months, maybe the monitored data still cannot reflect the response of the reservoir completely. Therefore, more production data (history) is needed to further confirm the reservoir model and calculate more accurate future predictions. However, based on the fitting of the data, the three-tank open model seems to be the best one for the reservoir (Figure 28). It is noteworthy that neither of these two models could simulate the second production step-test, which was accurately simulated by a two-tank open model as was shown in the well test section (Figures 23-26). It seems that the simulated models for different sets of test data are inconsistent with each other. The reason is, however, the different time-scales involved. The first and second production step-tests only lasted a short time, about 8 and 14 hours, respectively, resulting in a much smaller affected range (reservoir volume) than the long term production and recovery test which lasted about two and a half months.

The calculated permeability thickness is about 9 Dm for the first tank, 13 Dm for the second tank and 7 Dm for the third tank. The permeability thickness of the first tank has the same order of magnitude as the results from the first and second step-tests. This is a convincing result since the step tests lasted a short time, hence affecting the reservoir only briefly.

The result, that the innermost tank, the outer tank and the recharge tank have similar permeability thicknesses, indicates the validity of the assumed open model. The size estimation results (Table 9) indicate that the whole system is probably a mixture of confined and unconfined subsystems. The volumes and surface areas of the first and second tank seem to be implausibly small when calculated assuming only unconfined conditions, but for the third tank it can be a realistic estimation. So it may

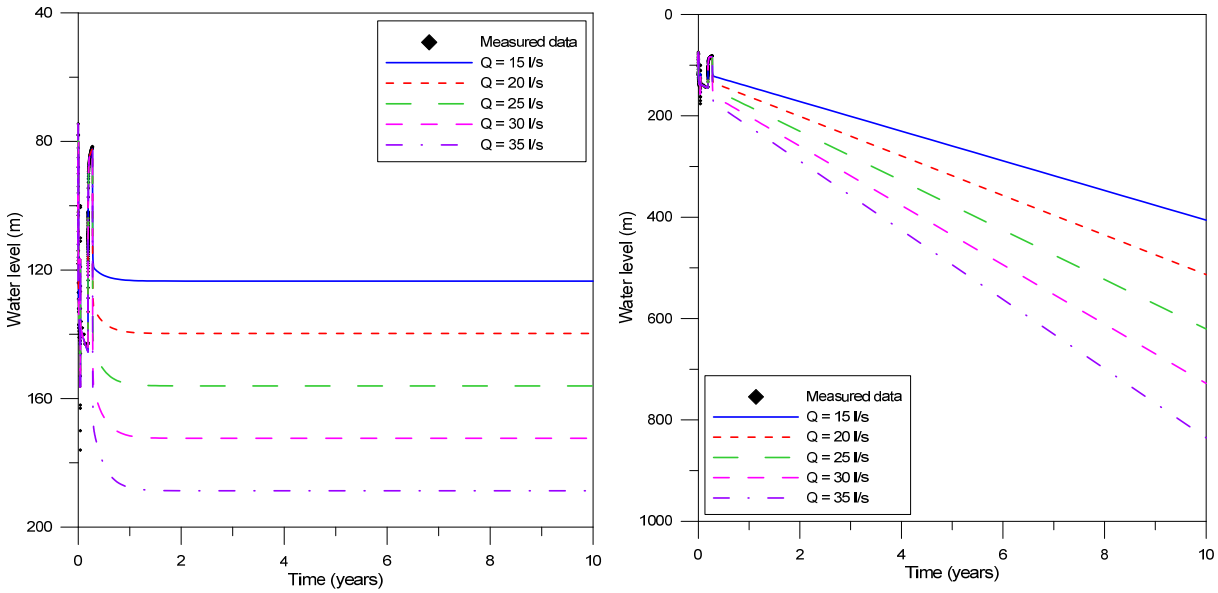

FIGURE 29: Predicted water levels in well SD-01 for the next 10 years for different production rates,

be concluded that the first and second tanks are mostly confined and the third tank is mostly unconfined in nature.

Future predictions calculated by the three-tank open model and three-tank closed model, were conducted at different rates (15, 20, 25, 30 and 35 L/s). The results (Figure 29) show that, in the following 10 years, the present production rate (25 L/s) cannot be maintained with a closed system since it leads to continuous decrease in the water level. A larger rate, such as 35 L/s, can be used to provide more geothermal water to local residents with an open system. From the prediction results, it seems that a completely closed system is unlikely but an open system is more likely. Reality will probably be somewhere between the two predictions. Then the water level for e.g. 20 L/s production is likely to be above 200-250 m depth, which is suitable for down-hole pumps. If the system is completely closed, then reinjection will be necessary, however.

6. CONCLUSIONS

Data from two step-tests and two and a half months of production test data as well as a month of build-up data from well SD-01 in Skarddalur, N-Iceland, were analysed with WellTester, LUMPFIT and the multiple rate test method. The future production response was predicted, as well, using LUMPFIT. Based on these results, it can be concluded that:

- The permeability thickness of the reservoir found using different methods is within the same order of magnitude, or around 10 Dm. The skin factor is between –1.2 and –1.5, the productivity index is around 5-6 (L/s)/bar and the reservoir thickness is estimated to range between 200 and 240 m.

- The parameters of the geothermal reservoir found by using the data from the first and second step-tests interpreted using WellTester, LUMPFIT and multiple rate test method are quite comparable.

- Based on the presently available long term production and build-up data, the best matching lumped parameter model is a three-tank open model; the inner parts of the reservoir seem to be

confined in nature while the outer and recharge parts of the system appear to be unconfined. The permeability thicknesses for each model tank are very similar.

- The temperature changed somewhat during the injection and production testing. The analysis in this report does not account for these temperature changes, which may lead to some bias. It is, therefore, recommended to use a non-isothermal lumped parameter model to fit and interpret the observed data in the future. No long-term temperature decline was observed, however.

- The pessimistic results show that, for a three-tank closed model, the present production rate (25 L/s) cannot be maintained for sustainable development and if the reservoir turns out to be completely closed, which is unlikely, reinjection may have to be applied in the future. On the other hand, the optimistic results show that, for a three-tank open model, a larger production rate than 25 L/s can be used to provide more geothermal water.

- Further measurements and assessments are necessary in the future to reveal the capacitance of the reservoir for sustainable development in this area. Careful and comprehensive monitoring once utilization starts is especially important.

ACKNOWLEDGEMENTS

I would like to express my gratitude to Dr. Ingvar B. Fridleifsson, director of the UNU Geothermal Training Program and Mr. Lúdvík S. Georgsson, deputy director, for giving me the great opportunity of attending this training and for excellent guidance. I would also like to thank Ms. Thórhildur Ísberg, Mr. Ingimar G. Haraldsson and Mr. Markús A.G. Wilde, for their assistance, hospitality and kindness, during the application for the fellowship and the period of training. I am most deeply and sincerely grateful to my supervisors, Dr. Svanbjörg H. Haraldsdóttir, Mr. Páll Jónsson and Dr. Gudni Axelsson, for their patient instruction and excellent guidance during my study. I thank the other fellows for our unforgettable friendship. I also thank RARIK (Iceland State Electricity) for permission to use the well data.

I am greatly indebted to my University and the Research Centre of Geothermal & Renewable Energy. I express my deepest thanks to Academician Wang Jiyang (Institute of Geology and Geophysics, Chinese Academy of Sciences), Professor Zha Ming (vice President of China University of Petroleum) and Professor Yao Jun (Dean of School of Petroleum Engineering, China University of Petroleum) for recommending me for this special training.

Finally, I am deeply grateful to my wife, He Yan, and my son, Liu Xinghe, for their love and support during these six months.

REFERENCES

Axelsson, G., 1989: Simulation of pressure response data from geothermal reservoir by lumped parameter models. *Proceedings of the 14th Workshop on Geothermal Reservoir Engineering, Stanford University, Stanford, Ca,* 257-263.

Axelsson, G., and Arason, Th., 1992: *LUMPFIT, automated simulation of pressure changes in hydrological reservoirs. Version 3.1, user´s guide*. Orkustofnun, Reykjavík, 32 pp.

Axelsson, G., Björnsson, G., and Quijano, J., 2005: Reliability of lumped parameter modelling of pressure changes in geothermal reservoirs. *Proceedings of the World Geothermal Congress 2005, Antalya, Turkey,* 8 pp.

Axelsson, G., Jónasson, T., Ólafsson, M., Egilsson, Th., and Ragnarsson, Á., 2010: Successful utilization of low-temperature geothermal resources in Iceland for district heating for 80 years. *Proceedings World Geothermal Congress 2010,* Bali, Indonesia, 25-29 April 2010, 8 pp.

Axelsson, G., and Ólafsson, M., 2010: *Status of geothermal production in Skútudalur in the spring 2010*. ÍSOR – Iceland GeoSurvey, Reykjavík, report ÍSOR-2010/021 (in Icelandic), 25 pp.

Bourdet, D., 2002: *Well test analysis: the use of advanced interpretation models*. Elsevier Science, 439 pp.

Horne, R.N., 1995: *Modern well test analysis, a computer aided approach* (2nd edition). Petroway Inc., USA, 257 pp.

Horne, R.N., 2010: *Geothermal well testing.* UNU-GTP, Iceland, unpublished lecture notes.

Jóhannesson, H., Kristinsson, S.G., and Jónasson, H., Tryggvason, H., Egilsson, Th., and Ólafsson, M., 2010: *Drilling of well SD-01 in Skarddalur in Siglufjördur – 2nd phase*. ÍSOR – Iceland GeoSurvey, Reykjavík, report ÍSOR-2010/036, 71 pp.

Jónsson, P., 2011: *Injection well testing*. UNU-GTP, Iceland, unpublised lecture notes.

Júlíusson, E., Jóhann, G., and Jónsson, P., 2007: *Well Tester 1.0b, user´s guide.* ÍSOR – Iceland GeoSurvey, Reykjavík, report ÍSOR-2008/063, 26 pp.

Kristinsson, S.G., and Egilsson, Th., 2010: *Production measurements on well SD-01 in Skarddalur in Siglufjördur*. ÍSOR – Iceland GeoSurvey, Reykjavík, report ÍSOR-2010/079 (in Icelandic), 21 pp.

Landmaelingar Íslands, 2011: *Map from database*. National Land Survey of Iceland. Webpage: *http://atlas.lmi.is/kortasja_en*/

Vitai, Z.M., 2010: *Sustainable use of low-temperature geothermal reservoirs in Iceland*. University of Iceland & University of Akureyri, School for Renewable Energy Science, MSc thesis, 95 pp.